# Morphology and Morphogenesis of SARS-CoV-2 in Vero-E6 cells

**Debora Ferreira Barreto Vieira** ( df.barreto@globo.com )
Instituto Oswaldo Cruz, Fundação Oswaldo Cruz

**Marcos Alexandre Nunes da Silva**
Instituto Oswaldo Cruz, Fundação Oswaldo Cruz

**Cristiana Couto Garcia**
Instituto Oswaldo Cruz, Fundação Oswaldo Cruz

**Milene Dias Miranda**
Instituto Oswaldo Cruz, Fundação Oswaldo Cruz

**Aline Rocha Matos**
Instituto Oswaldo Cruz, Fundação Oswaldo Cruz

**Braulia Caetano**
Instituto Oswaldo Cruz, Fundação Oswaldo Cruz

**Paola Cristina Resende**
Instituto Oswaldo Cruz, Fundação Oswaldo Cruz

**Fernando Mota**
Instituto Oswaldo Cruz, Fundação Oswaldo Cruz

**Marilda Mendonça Siqueira**
Instituto Oswaldo Cruz, Fundação Oswaldo Cruz

**Ortrud Monika Barth**
Instituto Oswaldo Cruz, Fundação Oswaldo Cruz

**Research Article**

**Keywords:** SARS-CoV-2, Vero-E6 cells, morphology, morphogenesis

**Posted Date:** July 9th, 2020

**DOI:** https://doi.org/10.21203/rs.3.rs-40432/v1

# Morphology and Morphogenesis of SARS-CoV-2 in Vero-E6 cells

Debora Ferreira Barreto-Vieira[1], Marcos Alexandre Nunes da Silva[1], Cristiana Couto Garcia[2], Milene Dias Miranda[2], Aline Rocha Matos [2], Braulia Caetano[2], Paola Cristina Resende[2], Fernando Motta [2], Marilda Mendonça Siqueira[2,] Ortrud Monika Barth[1]

[1]Laboratório de Morfologia e Morfogênese Viral, [2]Laboratório de Vírus Respiratórios e do Sarampo, Oswaldo Cruz Institute, Oswaldo Cruz Foundation.

Corresponding author: Debora Ferreira Barreto-Vieira (barreto@ioc.fiocruz.br)

**Abstract**

The coronaviruses (CoVs) called the attention of the world for causing outbreaks of severe acute respiratory syndrome (SARS-CoV), in Asia in 2002-03, and respiratory disease in the Middle East (MERS-CoV), in 2012. In December 2019, yet again a new coronavirus (SARS-CoV-2) first identified in Wuhan, China, was associated with a severe respiratory infection, known today as COVID-19. This new virus is highly transmissible, and quickly spread throughout China and 30 additional countries. As result, the World Health Organization (WHO) elevated the status of the COVID-19 outbreak from emergency of international concern to pandemic on March 11, 2020. The impact of COVID-19 on public health and economy fueled a worldwide race to approve therapeutic and prophylactic agents, but so far, there are no specific antiviral drugs or vaccines available. In current scenario, the development of *in vitro* systems for viral mass production and for testing antiviral and vaccine candidates proves to be an urgent matter. Research groups around the world are strongly focused on this, and the susceptibility of different cell lines to SARS-CoV-2 infection has already been demonstrated by molecular techniques. However, data on the biology of SARS-CoV-2 at the ultrastructural level in these *in vitro* models is still scarce. In this study, we documented, by transmission electron microscopy and real-time RT-PCR, the infection of Vero-E6 cells with SARS-CoV-2 samples isolated from Brazilian patients. The infected cells presented cytopathic effects and SARS-CoV-2 particles were observed attached to the cell surface and inside cytoplasmic vesicles. The entry of the virus into cells occurred through the endocytic pathway or by fusion of the viral envelope with the cell membrane. Assembled nucleocapsids were verified inside rough endoplasmic reticulum cisterns (RER). Viral maturation seemed to occur by budding of viral particles from the RER into smooth membrane vesicles. Therefore, the susceptibility of Vero-E6 cells to SARS-CoV-2 infection and the viral pathway inside the cells were demonstrated by ultrastructural analysis.

**Key Words:** SARS-CoV-2, Vero-E6 cells, morphology, morphogenesis

## Introduction

Coronavirus Disease 2019 (COVID-19) presents a clinical spectrum ranging from asymptomatic individuals to more complex conditions such as severe acute respiratory syndrome. Although most patients have mild symptoms and good prognosis, an estimate 10-20% of individuals may be developed the severe forms of illness, and 2-5% may die due complications in multiple organs. The pathogenesis of the disease related to the Severe Acute Respiratory Syndrome of Coronavirus 2 (SARS-CoV-2) in humans is still unclear (Lin et al., 2020). Among patients with pneumonia, fever was the most common symptom, followed by cough (Sun et al. 2020). Bilateral pulmonary involvement was the most common finding from chest computed tomography analysis (Lai et al., 2020). Dissemination of SARS-CoV-2 occurs mainly by person-to-person transmission, through contact with respiratory fluids. It is estimated that the infection has an average incubation period of six days.

COVID-19 was first identified in Wuhan, Hubei Province, Republic of China, on December 1st, 2019, but the initial reports only came out on December 31st of the same year. Since the early stages of the epidemics, several evidences have pointed to a probable zoonotic origin for SARS-CoV-2, in particular, the initial observation that first cluster of infections was linked to a seafood and live animal wholesale market. Since its isolation from Wuhan samples in January 2020 (Lu et al., 2020), SARV-CoV-2 has quickly spread in China and many other countries (Li et al., 2020; Gorbalenya et al., 2020; Chen et al., 2020; Huang et al., 2020; Wang et al., 2020; Holshue et al., 2020). On January 30th 2020, the WHO declared COVID-19 as the sixth public health emergency of international concern and, on March 11th 2020, raised the classification of SARS-CoV-2 outbreak to pandemic. By the time of the WHO announcement, more than 118,000 people had already been infected in 114 countries (https://www.who.int/docs/default-source/coronaviruse/situation-reports/20200311-sitrep-51-covid-19.pdf?sfvrsn=1ba62e57_10).

SARS-CoV-2 is an enveloped, positive-sense RNA virus belonging to genus Betacoronavirus (Chan et al., 2020; Lu et al.; 2020; Zhu el al., 2020). Phylogenetic analysis revealed that SARS-CoV-2 is closely related (88-89% similarity) to SARS-like coronaviruses from bats, such as bat-SL-CoVZC45 (GenBank no. MG772933.1) and bat-SL-CoVZXC21 (GenBank no. MG772934.1), and shares lower similarity to SARS-CoV (~79% similarity) and MERS-CoV (~50% similarity) [Lu et al, 2020; Jiang et al., 2020; Ren et al., 2020]. SARS-CoV-2 virions (infectious particles) have a diameter of approximately 50 to 200nm. Like in other coronaviruses, the SARS-CoV-2 lipid envelope contains a spike protein (S), a membrane

protein (M) and an envelope protein (E). The S protein mediates viral binding to the host cell membrane through interaction with the angiotensin conversion enzyme (ACE2) receptor (Hoffmann et al., 2020). The nucleocapsid protein (N) forms the virion core, which encases the viral RNA genome (Chen et al., 2020; Wu et al., 2020). Currently there are no specific antiviral drugs or vaccines for treating and preventing COVID-19. There are, though, several candidates in different stages of development, with few recently reaching the phases of clinical testing. Standardized in vitro systems for viral mass production and infection modeling are essential tools to accelerate the initial steps of drug development, screening and pre-clinical testing. In this sense, several research groups have demonstrated the susceptibility of different cell lines to SARS-CoV-2 through molecular techniques (Park et al., 2020; Harcout et al., 2020; Kim et al., 2020). However, studies regarding the morphogenesis of SARS-CoV-2 in cell lineages are scarce in the literature so far. Here, we used a lineage of African green monkey kidney cells (Vero-E6) to isolate SARS-CoV-2 viruses from samples of nasopharyngeal swabs of patients positive for COVID-19. Using transmission electron microscopy, we were able to document the morphology and replication cycle of SARV-CoV-2, and the consequent ultrastructural alterations induced in the host cells.

## Materials and Methods

*Clinical samples*

Nasopharyngeal swabs were collected from patients admitted to the sentinel health units of the national surveillance network for respiratory of the Brazilian MoH. Samples were obtained in different regions of the country and referred to the National Influenza Center (NIC) at Fiocruz, Rio de Janeiro for SARS-CoV-2 detection, as part of the COVID-19 surveillance program. Total RNA was extracted from clinical samples using the QIAmp Viral RNA mini kit (Qiagen). Viral detection was done by real time RT-PCR with TaqMan primers and probes (IDT) specific for the genes encoding the Envelope protein (E) and the viral RNA-dependent RNA Polymerase (RdRp), as described previously (Corman et al., 2020). Reactions were performed with the Qiagen One Step RT-PCR kit (Qiagen, USA). Synthetic RNA sequences corresponding to E and RdRP targets (Corman et al., 2020) were used as positive controls. Positive samples were then used for SARS-CoV-2 isolation in VERO E6 cells. This research is approved by Human Research Ethics Committee of Fundação Oswaldo Cruz, Instituto Oswaldo Cruz (protocol number 4.128.241).

*Cells and viral isolation*

All cell culture reagents were acquired from Gibco. Prior to infection, Vero-E6 (African green monkey kidney) cultures were maintained in DMEM supplemented with 10% fetal bovine serum (FBS) and 100U/mL of penicillin-streptomycin (1x Pen-Strep) and cultured at 37º C and 5% $CO_2$ (Szretter, 2006). For infection, monolayers were washed twice with PBS and inoculated with a clinical sample diluted in non-supplemented DMEM. Non-infected control cultures (mock) were prepared using pure non-supplemented DMEM as inoculum. After incubation for 1 hour at 37º C, the viral (and mock) inoculum was removed and cells were cultivated at 37º C in DMEM supplemented with 2% FBS and 1x Pen-Strep. Monolayers were inspected daily under light microscope for development of cytopathic effect (CPE), until 72 hours post infection (hpi). All procedures were performed in a biosafety level 3 laboratory, according to WHO guidelines. Whole-genome sequences of isolates evaluated in this study are available in the Global initiative on sharing all influenza data (GISAID) under the accession numbers EPI_ISL_415105, EPI_ISL_414045 e EPI_ISL_427294 (https://www.gisaid.org/).

*Viral quantification in cell cultures supernatants*

Viral quantities in cultures were estimated by determination of the number of copies of the viral gene E per volume (µL) of supernatant. Total RNA was extracted from culture supernatants using the QIAmp Viral RNA mini kit (Qiagen). Quantification of E gene copies was performed by real time RT-PCR using specific TaqMan primers and probes (Corman et al., 2020) and the Qiagen one step RT-PCR kit (Qiagen, USA). A standard curve was set using a synthetic RNA control containing the sequence of E gene. The control, with initial concentration from $10^8$ copies/µL, was serially diluted (with factor 10) to obtain a series of $10^7$ copies/µL to 10 copies/µL.

*Transmission electron microscope*

Infected and non-infected control (Mock) monolayers were trypsinized at 24, 48 and 72 hpi. Cell suspensions were fixed in 2.5% glutaraldehyde in sodium cacodilate buffer (0.2 M, pH 7.2), post-fixed in 1% buffered osmium tetroxide, dehydrated in acetone, embedded in epoxy resin and polymerized at 60˚C over the course of three days (Barreto-Vieira et al., 2010; Barth et al., 2016). Ultrathin sections (50–70 nm) were obtained from the resin blocks. The sections were picked up using copper grids, stained with uranyl acetate and lead citrate (Reynolds,

1963), and observed using Jeol JEM 1011 and FEI Tecnai T12 transmission electron microscopes.

## Results

*SARS-CoV-2 quantification from Vero-E6 cell culture supernatants*

To evaluate the ability of Vero-E6 cells to produce SARS-CoV-2 progeny, we quantified the number of copies of viral RNA in culture supernatants collected one and 72 hours post infection (hpi). The quantitative real time RT-PCR assay demonstrated an increase in the amount of SARS-CoV-2 RNA copies in the supernatant over three $\log_{10}$ steps within 72 hpi, from $1{,}2x10^4(\pm 6{,}7x10^4)$ to $1{,}4x10^7(\pm 1{,}6x10^6)$ copies/mL, suggesting productive viral infection.

*Morphological analysis of Vero-E6 cell cultures infected with SARS-CoV-2*

Analysis of cultures under inverted light microscopy demonstrated CPE in infected Vero-E6, which was mostly evident from 48 hpi. The CPE appeared as rounding and detaching of cells and formation of syncytia (data not shown).

Ultrastructural analyses of Vero-E6 cells at 72 hpi by transmission electron microscopy showed that the predominant changes associated to SARS-CoV-2 infection were, as follows: cell activation evidencing strong filopodia presence (Figures 1B and 1C), alteration and degeneration of mitochondria (Figures 2A-2D), an increased number of thickened ribosomes (Figure 2E), thickening of the nuclear membrane (data not shown) and RER (Figure 2A-2B, 2F and 6D), presence of clatrine vesicles (Figure 2F), smooth vesicle proliferation resulting in a severe vacuolization of the cells (Figures 3A-3D), numerous myelin figures (Figures 3E), and chromatin profile change in the nucleus (Figures 4A-4C). As compared with the infected cells, no ultrastructural changes were observed in the uninfected Vero cells (Figure 1A).

Virus particles attached to the cell surface (Figures 5A-5C and 5E) and envelopes fusing with the cell membrane (Figure 5H) could be observed. Entry of the SARS-CoV-2 virus particles into the cells was observed through fusion of the virus envelope with the cell membrane (Figure 5H) or by endocytosis (Figures 5D, 5F, 5G). Virus particles presented spherical morphology displaying spikes on its surface (Figure 5G), characteristic of viruses belonging to the *Coronaviridae* family and have an average diameter of 100nm. Nucleocapsids were observed inside in the swollen RER (Figures 6A-6C). The thickened ribosomes attached to the RER membrane were present at few numbers or disappeared completely (Figures 6A-6C).

Nucleocapsids were rarely observed associated with the nucleus membrane (Figure 4D). The virions were observed inside smooth vesicles at the periphery of the cell (Figures 6D-6F).

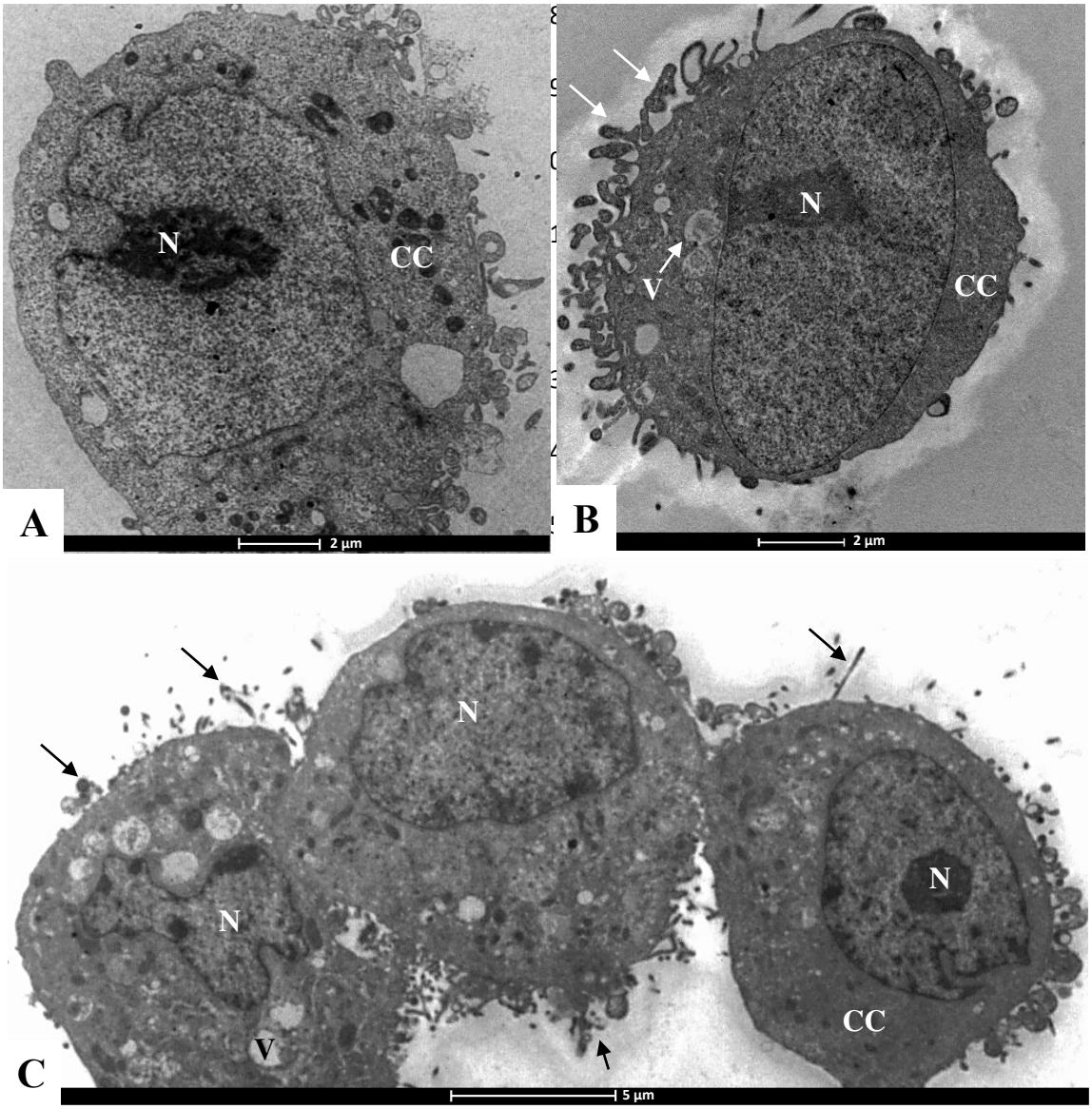


**Figure 1.** Ultrastructural analyses of Vero-E6 cells by transmission electron microscopy. [A]: Uninfected cell presenting no morphological alterations. [B-C]: Vero-E6 cells, 72hpi. with SARS-CoV-2, presenting numerous filopodia (arrows) and vesicles (V). Nucleus (N), cell cytoplasm (CC).

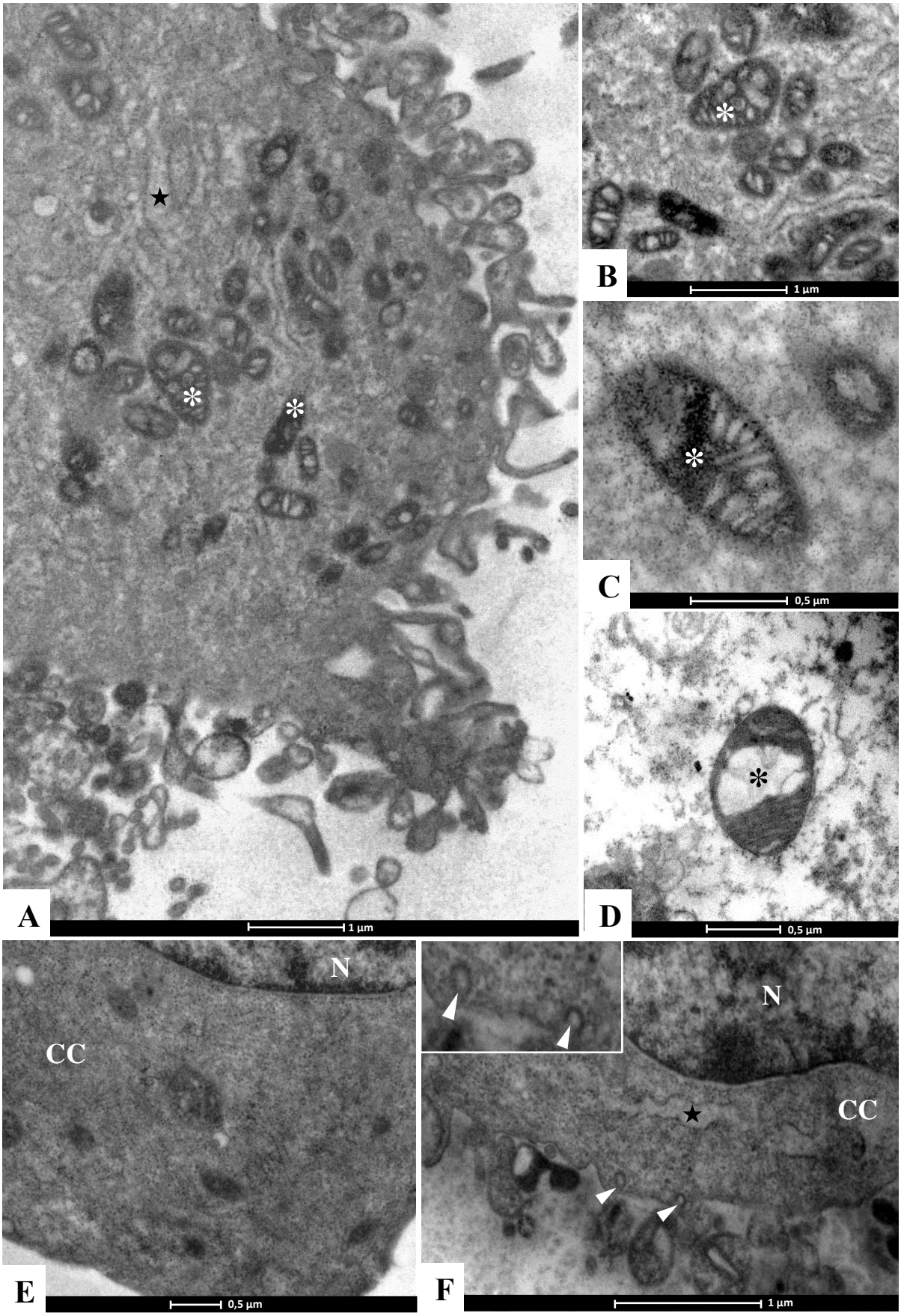


**Figure 2:** Ultrastructural alterations in Vero-E6 72hpi. with SARS-CoV-2. [A-D]: Alterations and degeneration of mitochondria (*). [E]: Cell cytoplasm (CC) of electron-dense aspect due

213 to thickening of the ribosomes. [A, F]: Thickening of the rough endoplasmic reticulum cistern
214 (star). [F]: Presence of clatrine vesicles (arrow heads, inset). Nucleus (N), cell cytoplasm (CC).

215

216

217

218

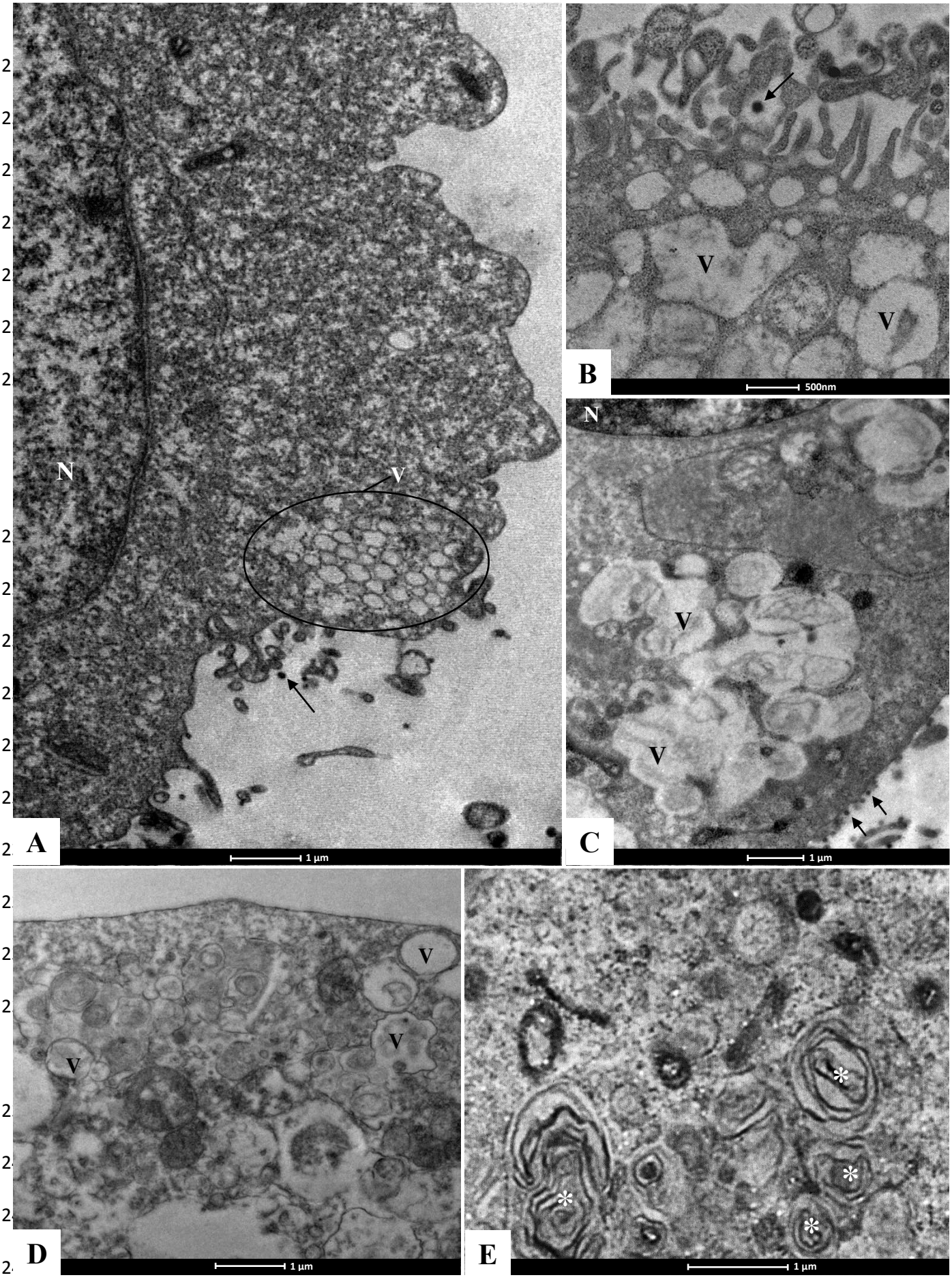
N
V
A
1 µm
V
V
B
500nm
N
V
V
C
1 µm
V
V
V
D
1 µm
E
1 µm

**Figure 3:** Intense smooth vesicle proliferation (V) in Vero-E6 72hpi with SARS-CoV-2. [A-D]: Vesicle (V) proliferation. Virus particle (B, arrow), nucleus (N). [E]: Cell cytoplasm presenting numerous myelin figures (*).

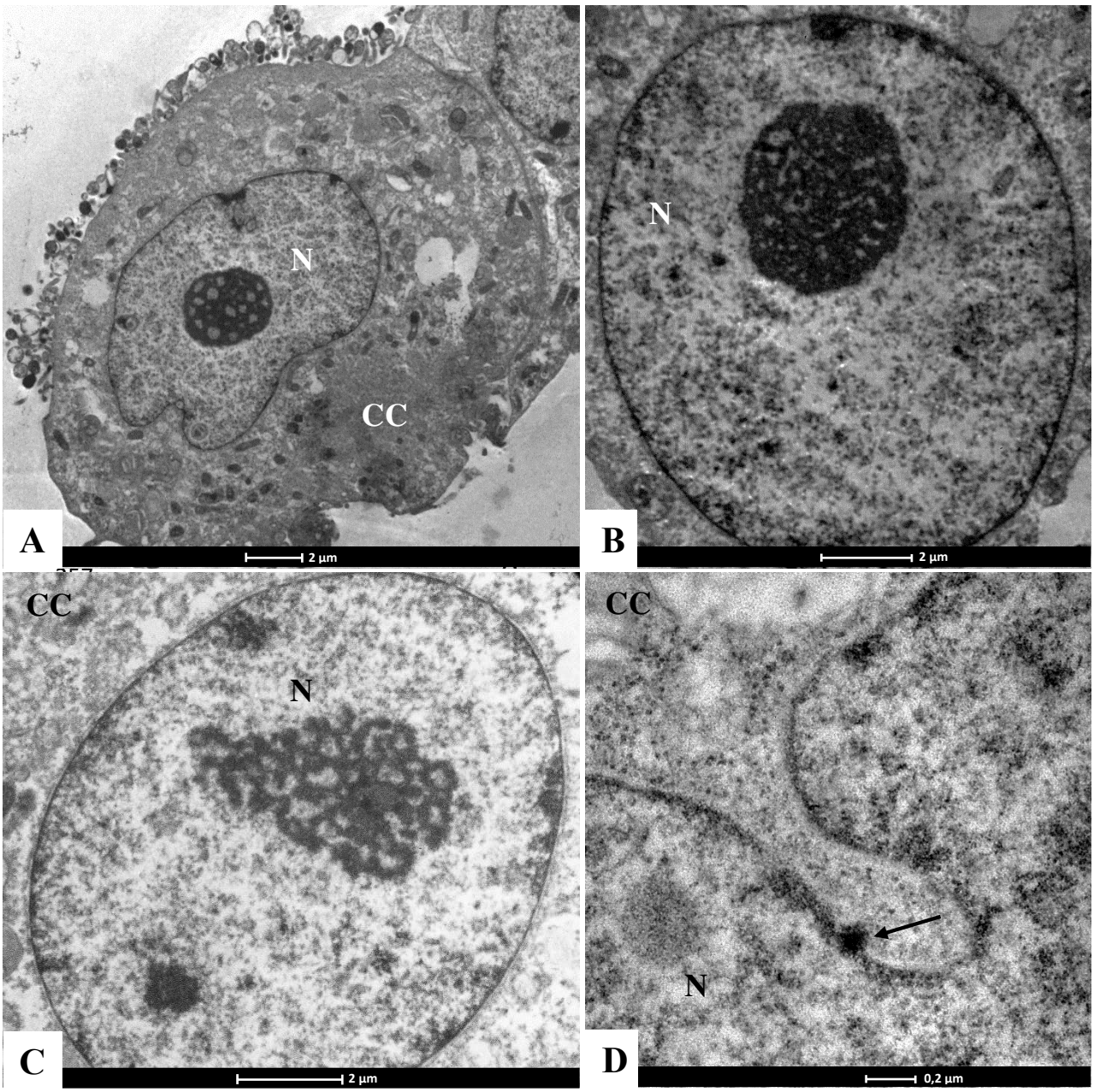


**Figure 4:** [A-C]: Alterations of the nucleus (N) chromatin profile in Vero-E6 72hpi with SARS-CoV-2. [D]: Viral nucleocapsid associated with the nucleus membrane (arrow). Cell cytoplasm (CC).

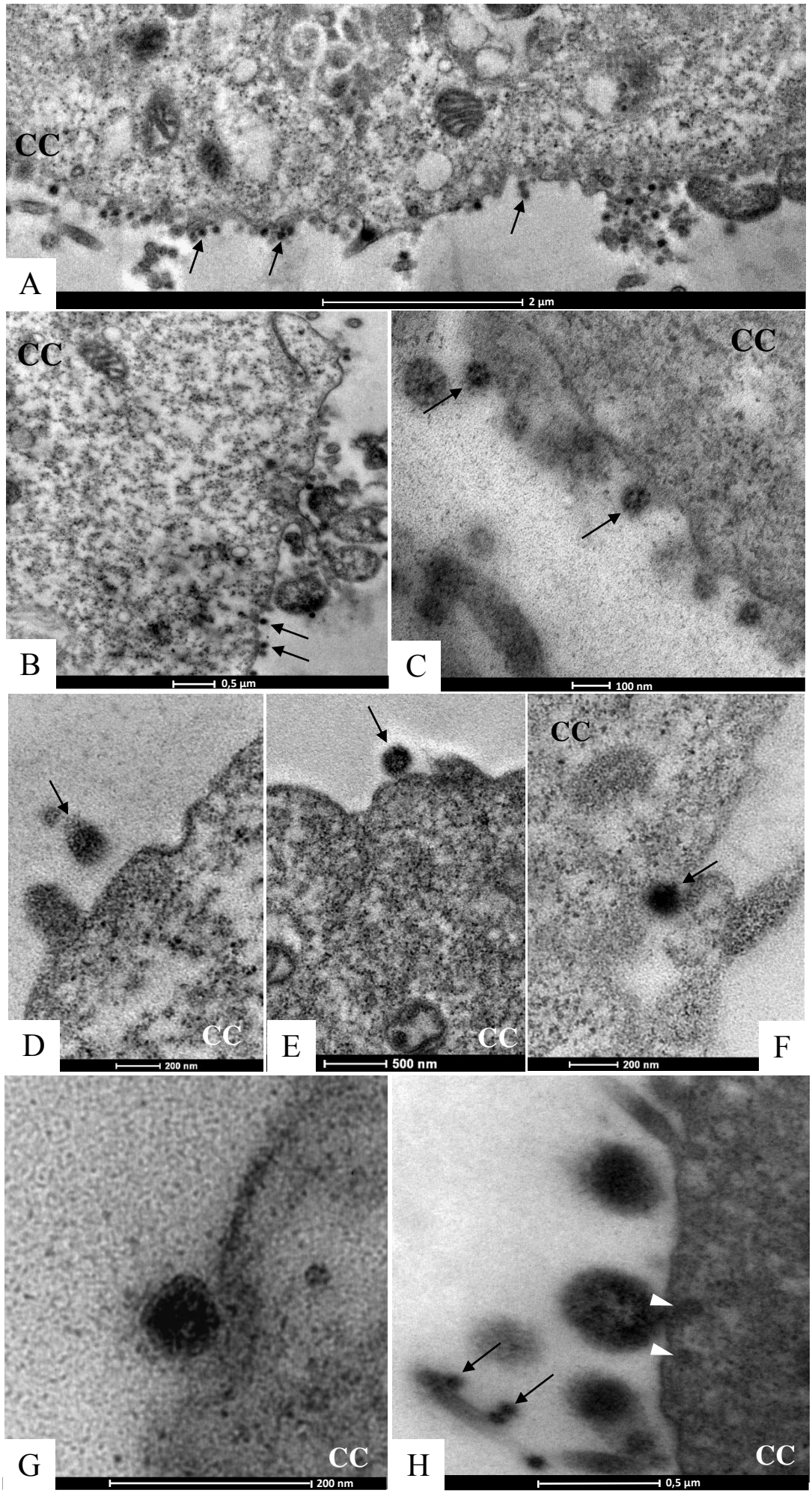
CC
A
2 µm
CC
B
0,5 µm
CC
C
100 nm
D
CC
200 nm
E
CC
500 nm
CC
F
200 nm
G
CC
200 nm
H
CC
0,5 µm

**Figure 5:** Attachment and entry of SARS-CoV-2 in Vero-E6 cells 72hpi [A, B, C, E]: Several virus particles (arrows) attached to cell membranes were observed. [D, F, G]: Entry of virus particles into cells by the endocytic pathway and by fusion of virus envelopes with cell membranes (head arrows) [G, H]: Virus particles presenting spherical morphology, displaying spikes, and an average diameter of 100nm. Cell cytoplasm (CC).

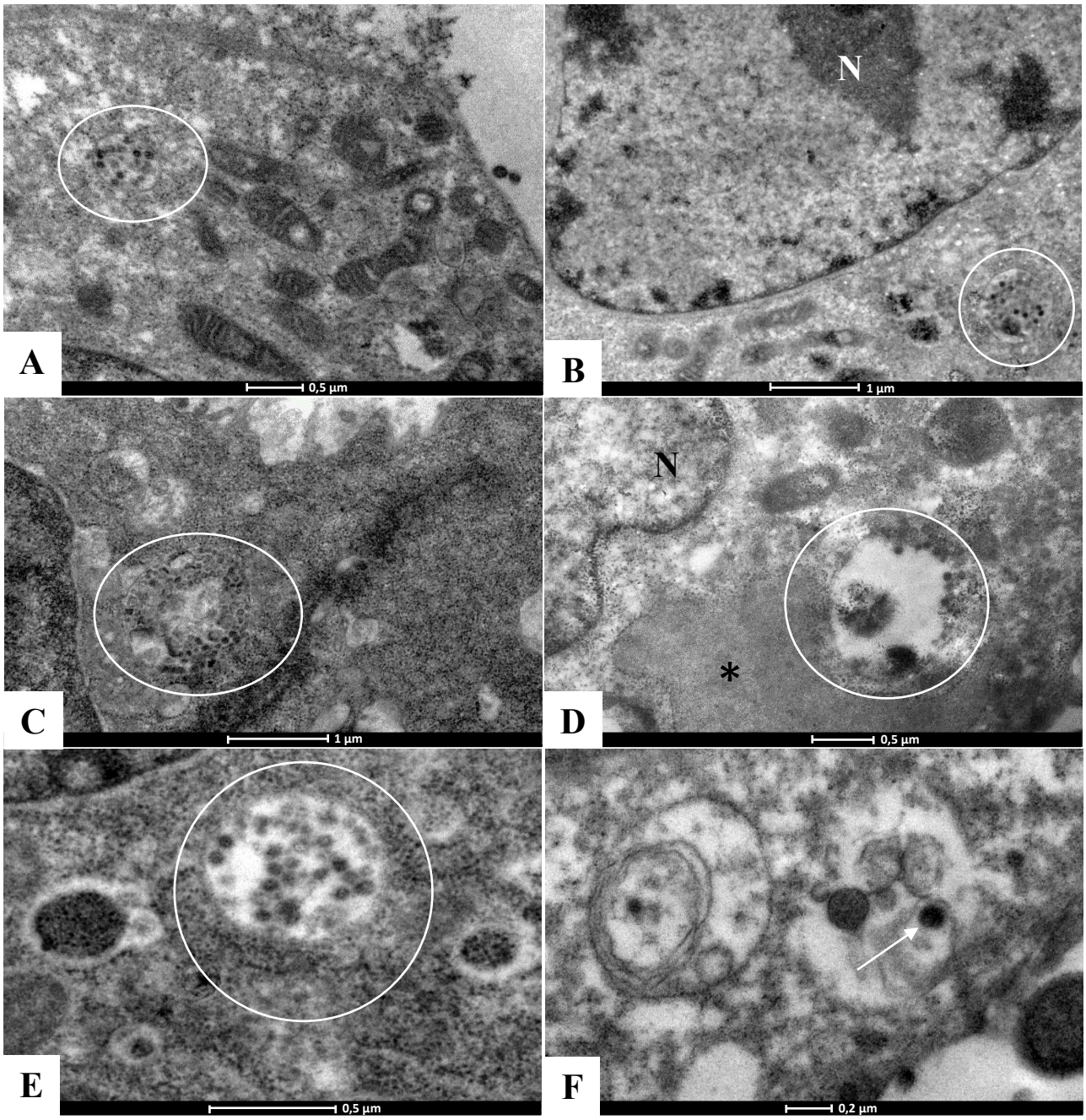


**Figure 6:** Morphogenesis of SARS-CoV-2 in Vero-E6 cells 72hpi [A, B, C]: Nucleocapsids inside swollen RER (circles). [D, E, F]: Virions were observed inside smooth vesicles at the periphery of the cell (circles and arrow). [D]: Thickening of a rough endoplasmic reticulum cistern (asterisk) including a dense electron matrix. Nucleus (N).

## Scheme of the Morphogenesis of the SARS-CoV-2

Based on ultrastructural analyses of Vero-E6 cells infected with SAR-Cov-2, we propose a scheme for the morphogenesis of the virus (Figure 7):

1. **Entry of the virus:** It may take place through the endocytic pathway **(A)** or by fusion of the viral envelope with the cell membrane **(B)**.
2. **Synthesis and assembly:** As only nucleocapsids were observed in cisterns of the RER **(C)**, we hypothesize that part of the assembly occurs in the RER. As a rare observation, nucleocapsids were found attached to the cell nucleus **(D)**, which suggests the participation of the nucleus in viral synthesis. Virions were observed only inside smooth vesicles **(E)** located in the peripheral part of the cell, suggesting that the nucleocapsids acquire the envelopes by budding from the RER into these vesicles.
3. **Release of viral progeny:** Given the location of the vesicles containing the virions, it is possible that the release of the viral progeny occurs throughout the fusion of the smooth vesicles with the cell membrane **(F)**.

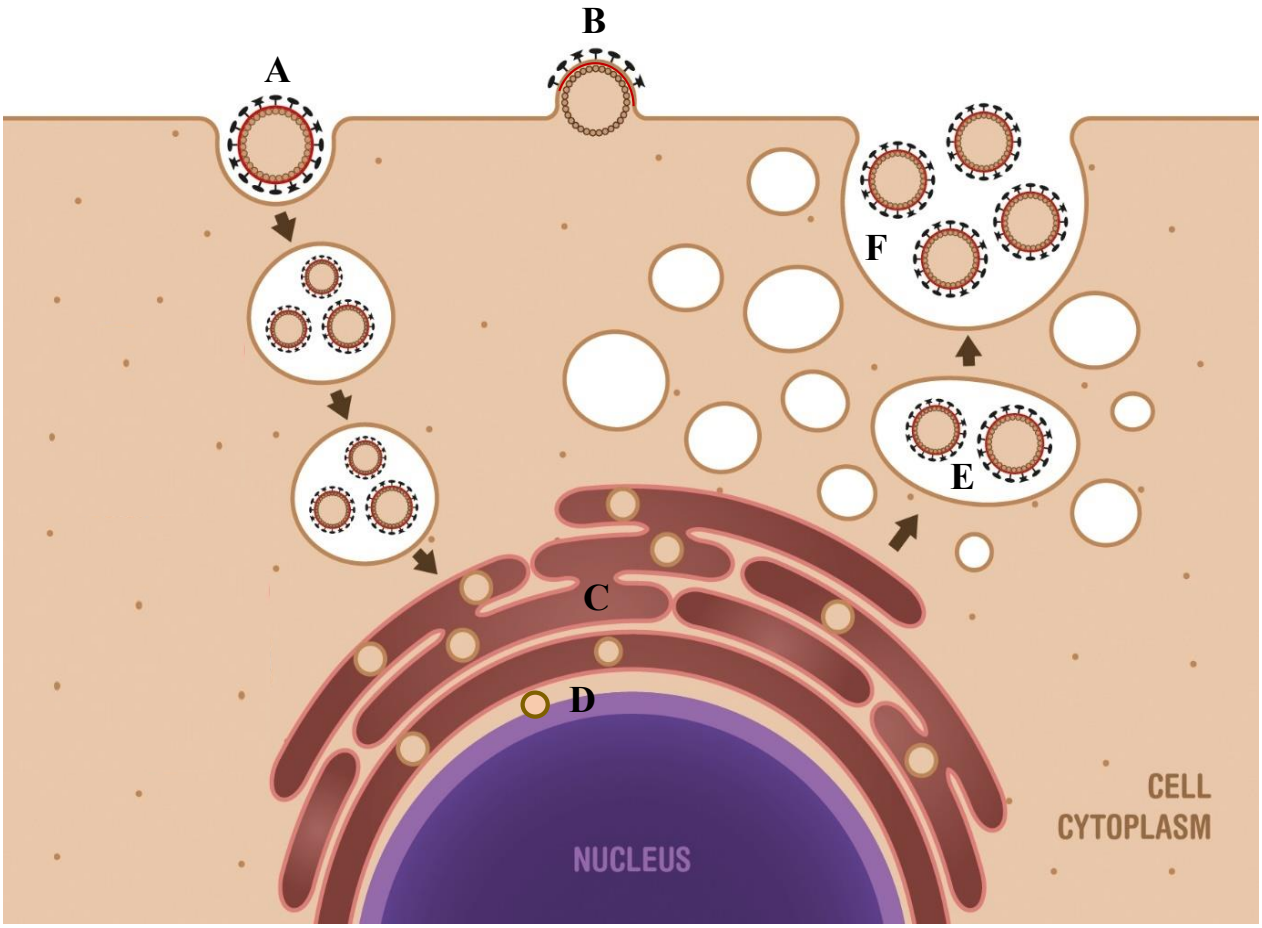


**Figure 7:** Suggested steps of SARS-CoV-2 morphogenesis in Vero-E6 cell

## Discussion

In the present study, using different parameters, we were able to show that Vero-E6 cells are highly permissive to SARS-CoV-2 replication. We observed a logarithmic increase in the number of viral RNA copies in cell culture supernatants, the display of a characteristic cytopathic effect in cell monolayers, and profound alterations in cell ultrastructure, as well as accumulation of viral components and viral particles in different cell compartments and times after infection. These data corroborate those of Park et al. (2020) and Harcourt et al. (2020) that described the susceptibility of this cell lineage for SARS-CoV-2 infection. These authors suggest that Vero-E6 cells might be the best choice for amplification and quantification of the virus. Transmission electron microscopy showed that the predominant changes associated to SARS-CoV-2 infection were cell activation, alteration of mitochondria, thickening of the RER and smooth vesicle proliferation, resulting in a severe vacuolization of the cells. Our findings are corroborated by the studies carried out by Qinfen et al. (2004) with SARS-CoV, which also observed that, as the infection progresses, the smooth vesicles increased both in number and size. However, while these authors concluded that the smooth vesicles were derived from the Golgi apparatus, our results suggest that they may be related to the RER.

To our knowledge, this is the first ultrastructural characterization of the morphogenesis of SARS-CoV-2 during viral replication in a cellular model. Our analysis suggest that viral entry into the host cell could occur either by endocytosis or by fusion of the viral envelope with the cell membrane. This is consistent with information from literature, in which we could find studies supporting both mechanisms (Song et al., 2019; Qinfen et al., 2004; Ng et al., 2003). Nucleocapsids were observed inside RER cisterns, which presented thickening with a dense electron matrix and gradual loss of ribosomes. This indicates that part of the SARS-CoV-2 protein synthesis and assembly may occur in the RER. Studies conducted by Zhang et al. (2003a) and Qinfen et al. (2004) pointed that the core of SARS-CoV is initially assembled in the RER, where the N protein binds to the genomic RNA and forms the nucleocapsid. The RER gradually loses the ribosomes and swells to become the matrix vesicles that contain the viruses. Qinfen et al. (2004) observed SARS-CoV-like particles in the nucleus of Vero-E6 cells at 48 hpi. Moreover, the nucleic membrane, being in connection with the RER, swelled to form blebs that contained nucleocapsids. These blebs were seen to detach from the nucleic membrane and turn into the virus morphogenesis matrix vesicles.

The presence of virions exclusively inside cytoplasmic smooth vesicles indicates that the particles acquire their envelopes are delivered by budding from the RER directly into smooth vesicles. This process is consistent with those observed with other coronaviruses. Qinfen et al. (2004) demonstrated that the SARS-CoV viral nucleocapsids sprout during morphogenesis from matrix vesicles into these smooth vesicles. In the last step of viral morphogenesis, we observed the virion filled smooth vesicles accumulating in the periphery of the cytoplasm, close to the cell membrane. Subsequent release of viral progeny occurred through the fusion of smooth vesicles with the cell membrane. Similar release mechanisms were described for SARS-CoV, which was also shown to accumulate inside smooth vesicles that move to the cell periphery and eventually fuse with the cell membrane (Qinfen et al., 2004). The mature SARS-CoV-2 virions had a spherical morphology, an average diameter of 100nm, and presented the characteristic spikes on the envelopes, which is the signature morphological feature of the coronaviruses. Again, our findings are very consistent with previous in vitro studies with SARS-CoV (Qinfen et al., 2004) and SARS-CoV-2, although the last one was reported to present some pleomorphism, and a wider range of virion diameter that varied from 50 to 200nm (Zhu et al., 2020; Park et al., 2020; Chen et al., 2020; Wu et al., 2020).

Further immunomicroscopy and tomography studies are needed to get a better design of the SARS-CoV-2 replication cycle, to better understand the role of the core of SARS-CoV-2 synthesis. The data presented in the present study are important for use in the development of model systems to evaluate therapeutic approaches.

**ACKNOWLEDGEMENTS**

We thank Dra. Suzana Corte Real and Dr. Wendell Girard Dias (Rudolph Barth Microscopy Platform, Oswaldo Cruz Institute, Fiocruz) and Jefferson Mendes de Miranda (SEJOR, Oswaldo Cruz Institute, Fiocruz) for technical assistance, NB3 Platform (Oswaldo Cruz Institute, Fiocruz) and CENABIO, Federal University of Rio de Janeiro, Brazil.

## References


Barreto-Vieira, D.F., Barth-Schatzmayr, O.M. & Schatzmayr, H.G. (2010). Modelo animal experimental para o estudo da patogênese dos vírus dengue sorotipos 1 e 2, manual de técnicas. Interciência, Rio de Janeiro, 82. p.

Barth, O.M., da Silva M.A.N. & Barreto-Vieira, D.F. Low impact to fixed cell processing aiming transmission electron microscopy. *Mem. Inst. Oswaldo Cruz,* **111(6)**:411–413 (2016).

Corman, V.M., et al. Detection of 2019 novel coronavirus (2019-nCoV) by real-time RT-PCR. Euro Surveill., **25(3)**:1–8 (2020).

Chan, J.F., et al. Genomic characterization of the 2019 novel human-pathogenic coronavirus isolated from a patient with atypical pneumonia after visiting Wuhan. *Emerg. Microbes Infect.,* **9**:221-236 (2020).

Chen, N., et al. Epidemiological and clinical characteristics of 99 cases of 2019 novel coronavirus pneumonia in Wuhan, China: a descriptive study. *Lancet*, **395**:507-513 (2020).

Gorbalenya, A.E. et al. Severe acute respiratory syndrome-related coronavirus: the species and its viruses—a statement of the Coronavirus Study. Group bioRxiv (2020 Feb 11), 10.1101/2020.02.07.937862.

Harcourt, J. et al. Severe Acute Respiratory Syndrome Coronavirus 2 from Patient with 2019 Novel Coronavirus Disease, United States**.** *Emerg. Infect. Dis*., **26(6)** (2020).

Holshue, M.L., et al. First case of 2019 novel coronavirus in the United States. N. Engl. J. Med. (2020 Jan 31), 10.1056/NEJMoa2001191.

Huang, C., et al. Clinical features of patients infected with 2019 novel coronavirus in Wuhan, China. *Lancet*, **395**:497-506 (2020).

Jiang, S., Du, L. & Shi, Z. An emerging coronavirus causing pneumonia outbreak in Wuhan, China: calling for developing therapeutic and prophylactic strategies. *Emerg. Microbes Infect.*, **9**:275-277 (2020).

Kim, J.M., et al. Identification of Coronavirus Isolated from a Patient in Korea with COVID-19. *Osong Public Health Res. Perspect.,* **11(1)**:3-7 (2020).

Lai, C.C., Tzu-Ping, S., Wen-ChienKo, H.J., & Po-RenHsueh. Severe acute respiratory syndrome coronavirus 2 (SARS-CoV-2) and coronavirus disease-2019 (COVID-19): The epidemic and the challenges. *Int. J. Antimicrob. Ag*., **55** (2020).

Li, Q., et al. Early transmission dynamics in Wuhan, China, of novel coronavirus-infected pneumonia. *N. Engl. J. Med.* (2020 Jan 29), 10.1056/NEJMoa2001316.

Lin, et al. 2020. Hypothesis for potential pathogenesis of SARS-CoV-2 infection -a review of immune changes in patients with viral pneumonia. *Emerg Microbes Infect*., **9(1)**:727-732 (2020)

Lu, H., Stratton, C.W. & Tang, Y.W. Outbreak of pneumonia of unknown etiology in Wuhan China: the mystery and the miracle. *J. Med. Virol.* (2020 Jan 16), 10.1002/jmv.25678.

Lu, R., et al. Genomic characterization and epidemiology of 2019 novel coronavirus: implications for virus origins and receptor binding. *Lancet,* **(20)**30251-8 (2020).

Ng, M.L., Tan, S.H., See, E.E., Ooi, E.E. & Ling, A.E. Early events of SARS coronavirus infection in Vero cells. J. Med. Virol., **71**: 323–331 (2003).

Park, W.B., et al. Virus Isolation from the First Patient with SARS-CoV-2 in Korea. *J. Korean Med. Sci*., **35(7)**:e84 (2020).

Qinfen, Z., et al. The life cycle of SARS coronavirus in Vero E6 cells. J. Med. Virol., **73(3)**:332-7 (2004).

Ren, L.L., et al. Identification of a novel coronavirus causing severe pneumonia in human: a descriptive study. *Chin. Med. J. (Engl)*, **133(9)**:1015-1024 (2020).

Reynolds, E.S. The use of lead citrate at high pH as an electron-opaque stain in electron microscopy. *J. Cell Biol.,***17**:208-12 (1963).

Song, Z., et al. From SARS to MERS, Thrusting Coronaviruses into the Spotlight. Viruses, 11(**1**): 59 (2019).

Sun, P., Qie, S., Liu, Z., Ren, J., Li, K., Xi, J. Clinical characteristics of 50 466 hospitalized patients with 2019-nCoV infection. J Med Virol [Internet]. 2020 Mar 11;jmv.25735. Available from: https://onlinelibrary.wiley.com/doi/abs/10.1002/jmv.25735

Szretter, K.J., Balish, A.L. & Katz, J.M. Influenza: propagation, quantification, and storage. *Curr. Protoc. Microbiol.* Chapter 15, Unit 15G 1 (2006).

Wang, C. P.W., Horby, F.G. & Hayden, G.F. A novel coronavirus outbreak of global health concern. *Lancet*, **395**:470-473 (2020).

Wu, C., et al. Analysis of therapeutic targets for SARS-CoV-2 and discovery of potential drugs by computational methods. *Acta Pharm. Sin. B*. 2020 Feb 27. doi: 10.1016/j.apsb.2020.02.008.

Zhang, Q., et al. Morphology and morphogenesis of severe acute respiratory syndrome (SARS)- associated virus. Acta Bioch. Bioph. Sin., **35**: 587–591(2003a).

Zhu, N., et al. A novel coronavirus from patients with pneumonia in China, 2019. N Engl J Med (2020 Jan 24), 10.1056/NEJMoa2001017.

# Figures

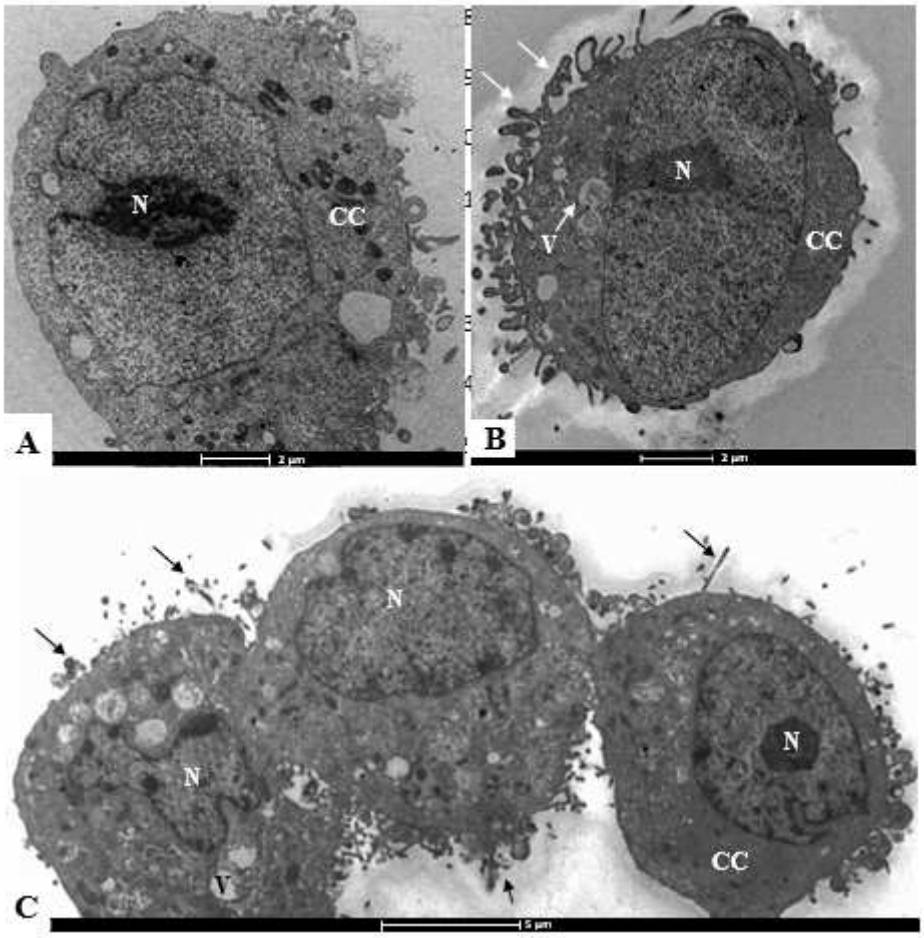


**Figure 1**

Ultrastructural analyses of Vero-E6 cells by transmission electron microscopy. [A]: Uninfected cell presenting no morphological alterations. [B-C]: Vero-E6 cells, 72hpi. with SARS-CoV-2, presenting numerous filopodia (arrows) and vesicles (V). Nucleus (N), cell cytoplasm (CC).

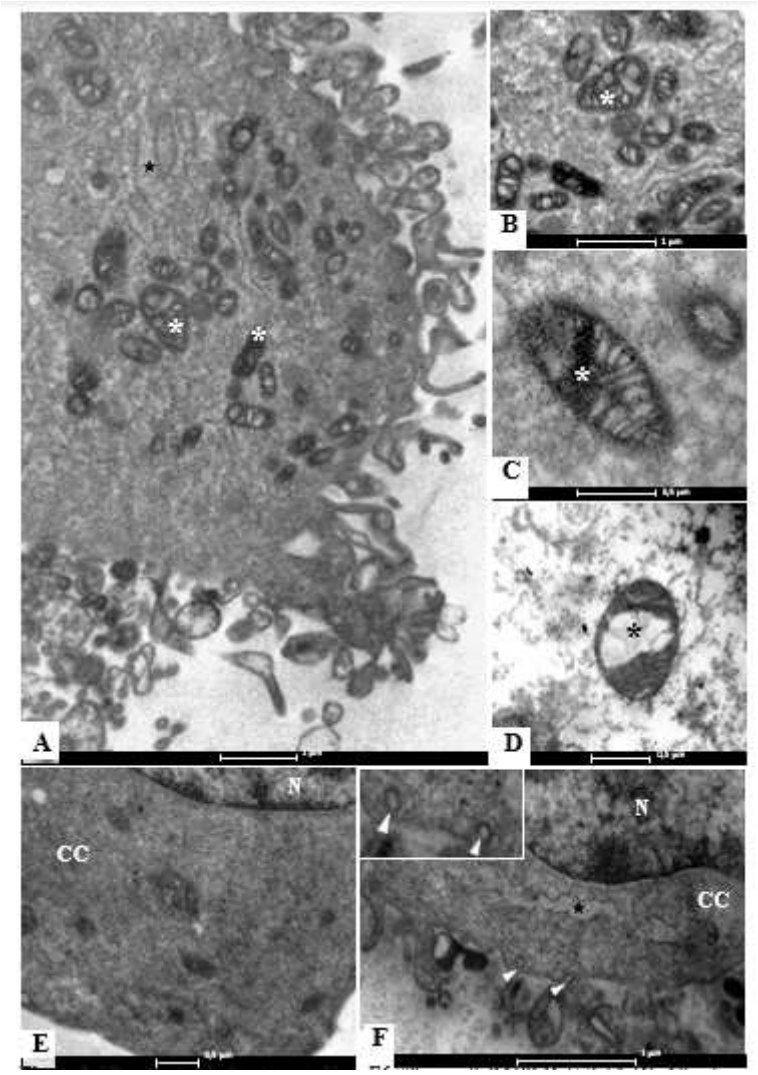


## Figure 2

Ultrastructural alterations in Vero-E6 72hpi. with SARS-CoV-2. [A-D]: Alterations and degeneration of mitochondria (*). [E]: Cell cytoplasm (CC) of electron-dense aspect due to thickening of the ribosomes. [A, F]: Thickening of the rough endoplasmic reticulum cistern (star). [F]: Presence of clatrine vesicles (arrow heads, inset). Nucleus (N), cell cytoplasm (CC).

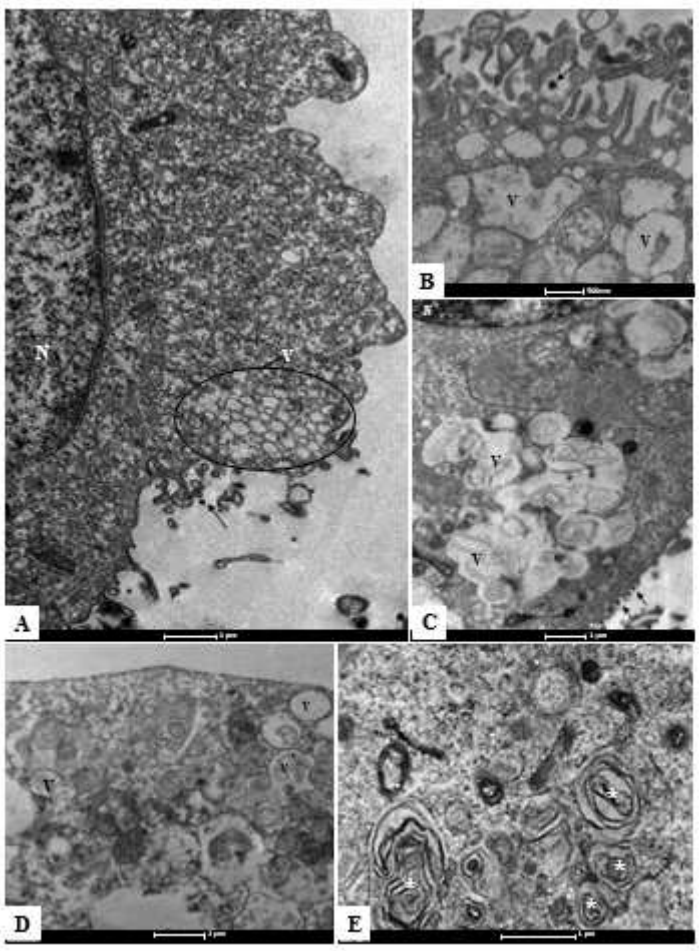


## Figure 3

Intense smooth vesicle proliferation (V) in Vero-E6 72hpi with SARS-CoV-2. [A- D]: Vesicle (V) proliferation. Virus particle (B, arrow), nucleus (N). [E]: Cell cytoplasm presenting numerous myelin figures (*).

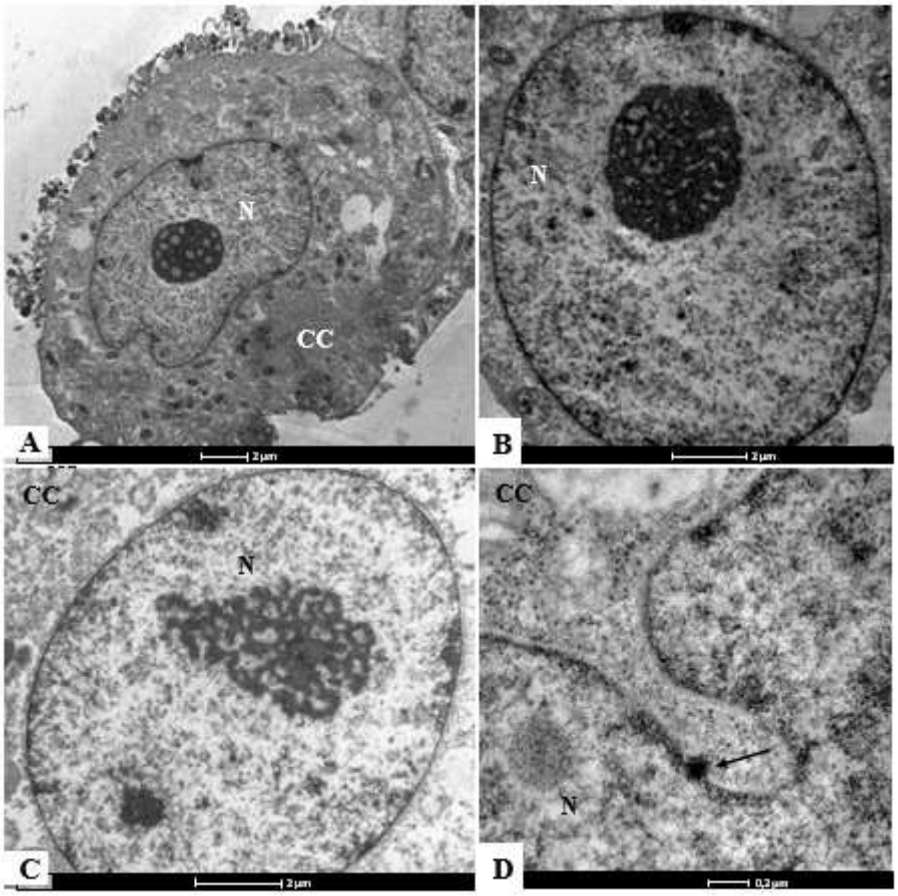


## Figure 4

[A-C]: Alterations of the nucleus (N) chromatin profile in Vero-E6 72hpi with SARS-CoV-2. [D]: Viral nucleocapsid associated with the nucleus membrane (arrow). Cell cytoplasm (CC).

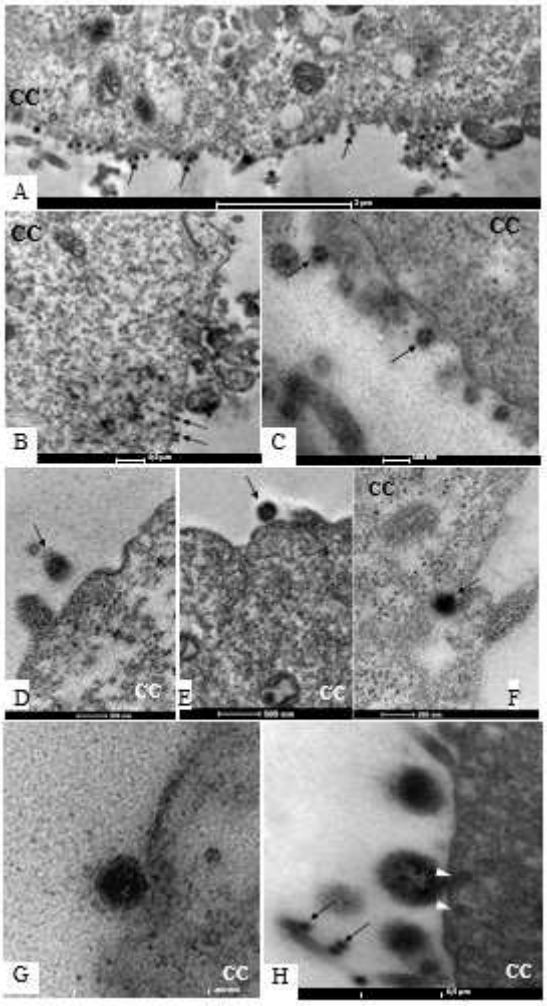


## Figure 5

Attachment and entry of SARS-CoV-2 in Vero-E6 cells 72hpi [A, B, C, E]: Several virus particles (arrows) attached to cell membranes were observed. [D, F, G]: Entry of virus particles into cells by the endocytic pathway and by fusion of virus envelopes with cell membranes (head arrows) [G, H]: Virus particles presenting spherical morphology, displaying spikes, and an average diameter of 100nm. Cell cytoplasm (CC).

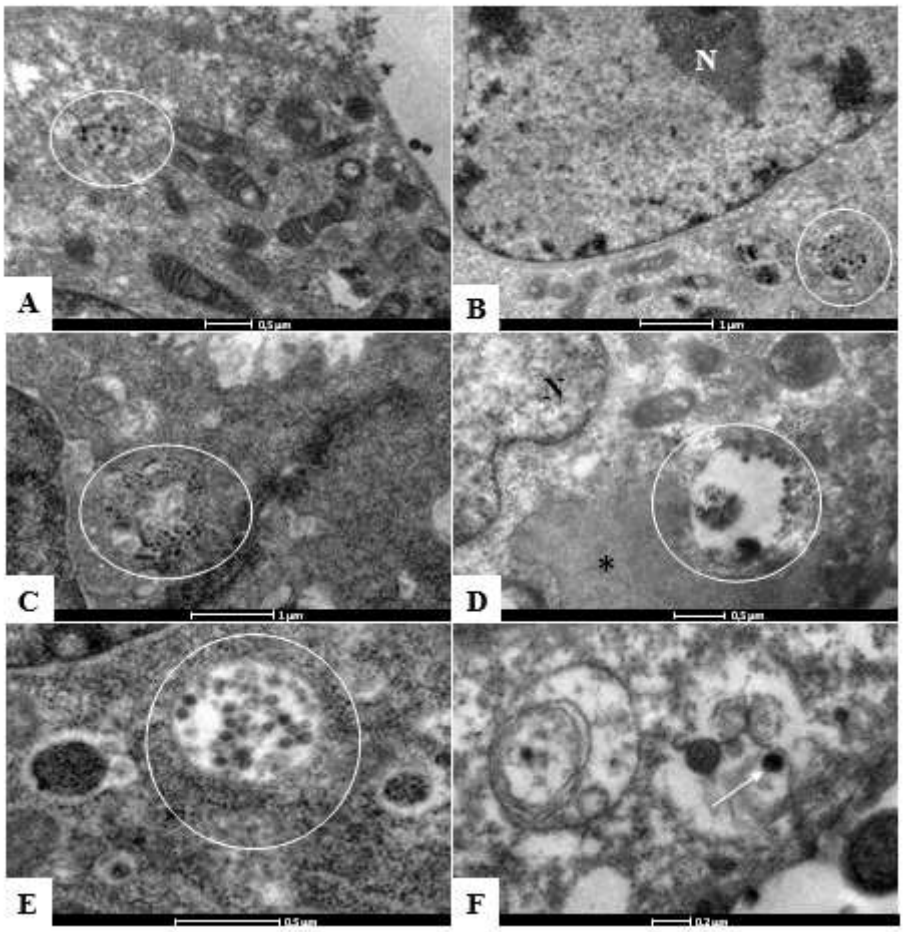


## Figure 6

Morphogenesis of SARS-CoV-2 in Vero-E6 cells 72hpi [A, B, C]: Nucleocapsids inside swollen RER (circles). [D, E, F]: Virions were observed inside smooth vesicles at the periphery of the cell (circles and arrow). [D]: Thickening of a rough endoplasmic reticulum cistern (asterisk) including a dense electron matrix. Nucleus (N).

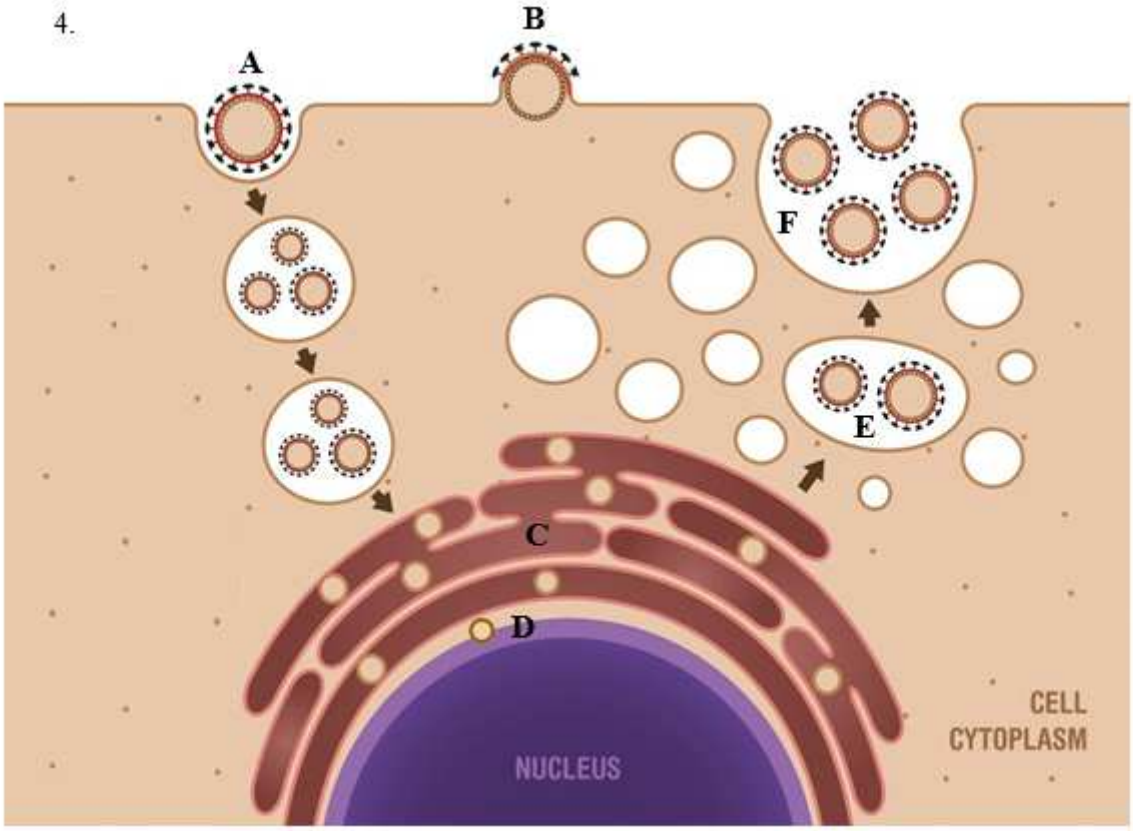


**Figure 7**

Suggested steps of SARS-CoV-2 morphogenesis in Vero-E6 cell